

Evidence from Identified Particles for Active Quark and Gluon Degrees of Freedom

Paul Sorensen

Brookhaven National Laboratory, P.O. Box 5000, Upton, NY 11973

E-mail: prsorensen@bnl.gov

Abstract. Measurements of intermediate p_T ($1.5 < p_T < 5.0$ GeV/c) identified particle distributions in heavy ion collisions at SPS and RHIC energies display striking dependencies on the number of constituent quarks in the corresponding hadron. One finds that elliptic flow at intermediate p_T follows a constituent quark scaling law as predicted by models of hadron formation through coalescence. In addition, baryon production is also found to increase with event multiplicity much faster than meson production. The rate of increase is similar for all baryons, and seemingly independent of mass. This indicates that the number of constituent quarks determines the multiplicity dependence of identified hadron production at intermediate p_T . We review these measurements and interpret the experimental findings.

PACS numbers: 25.75.-q, 25.75.Ld

Submitted to: *J. Phys. G: Nucl. Phys.*

1. Introduction

Physicists at the Relativistic Heavy Ion Collider (RHIC) have made several unexpected and potentially interesting observations [1]. Measurements relating to baryon production in the intermediate transverse momentum region ($1.5 < p_T < 5$ GeV/c) are one of those [2, 3, 4]. In p+p collisions at $p_T = 3$ GeV/c, one baryon is produced for every three mesons (1:3). In central Au+Au collisions however, baryons and mesons are created in nearly equal proportion (1:1). At this same p_T , the elliptic anisotropy (v_2) of baryons is also 50% larger than meson elliptic flow: demonstrating that baryon production is also enhanced in the direction of the impact vector between the colliding nuclei (in-plane) [3, 5]. The enhancement persists up to $p_T = 5.5$ GeV/c.

This effect is generic to many systems; baryon production is enhanced in systems that yield larger multiplicity and have the potential for an increase in multi-parton effects. Several possible explanations for the baryon enhancement are commonly considered:

Multi-quark or gluon processes during hadron formation—*coalescence* [6].

Gluon configurations that carry baryon number—*baryon junctions* [7, 8].

Collective motion amongst more massive baryons that populates the higher p_T regions of baryon p_T spectra—*flow* [9].

Coalescence models have garnered particular attention because they seem to provide a natural explanation for the constituent-quark-number scaling that has been observed in v_2 measurements. They also relate hadronic observables to a pre-hadronic stage of interacting quarks and gluons. As such, they touch on questions central to the heavy-ion physics program: deconfinement and chiral symmetry restoration. Given the potential physics benefits that can be derived from these measurements, experimentalists at RHIC and SPS have endeavored to extend their abilities to identify hadron types up to higher p_T regions [10]. Here I review those measurements which provide evidence for active quark and gluon degrees-of-freedom and discuss implications of the baryon enhancement on pion and non-photonic electron spectra.

2. Baryon to Meson Ratios

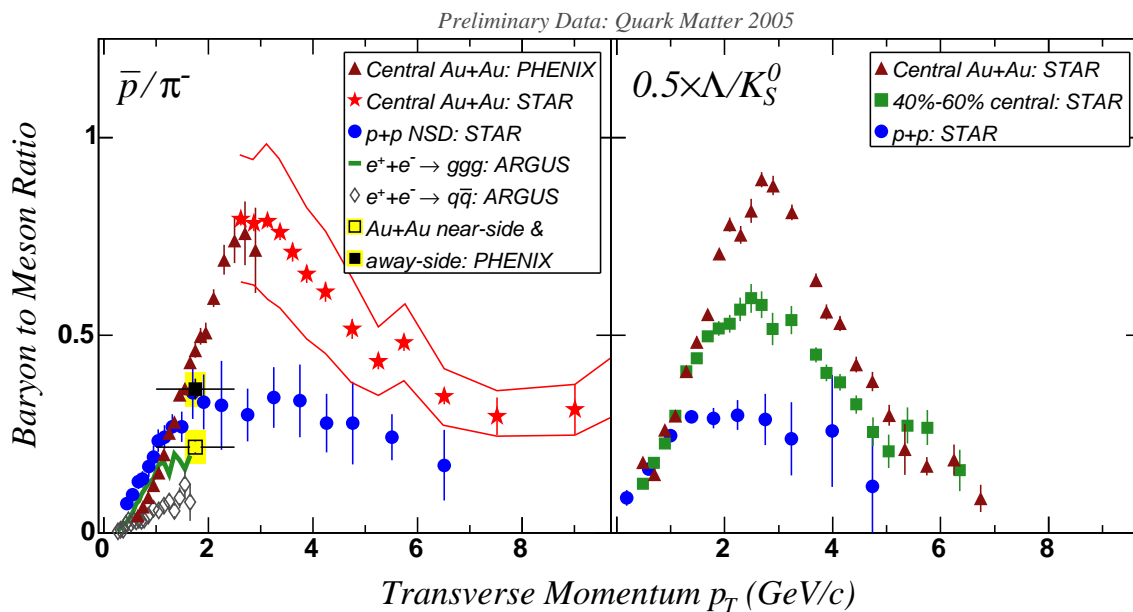


Figure 1. Left panel: the \bar{p}/π^- ratio at middle rapidity for central Au+Au and p+p collisions at $\sqrt{s_{NN}} = 200$ GeV. ARGUS measurements of the proton to pion ratio in e^+e^- collisions at $\sqrt{s} = 10$ GeV are shown for two classes of events: $e^+e^- \rightarrow \Upsilon \rightarrow ggg$ and continuum events dominated by $e^+e^- \rightarrow q\bar{q}$. Measurements of the proton to pion ratio made for particles associated with a trigger hadron ($p_T > 2.5$) are also shown [11]. Right panel: Λ/K_S^0 in central Au+Au, mid-peripheral Au+Au and minimum-bias p+p collisions [14]. Values are scaled by 0.5.

Figure 1 (left panel) shows the \bar{p}/π^- ratio measured in e^+e^- [12], p+p [13], and Au+Au [2, 13] collisions. The right panel shows the Λ/K_S^0 ratio for p+p, mid-peripheral

Au+Au, and central Au+Au collisions scaled by 0.5 [14]. In central Au+Au collisions, \bar{p}/π^- reaches a maximum value of nearly 1 at $p_T \approx 3$ GeV/c. The baryon junction calculations in Ref. [8] predict that the p_T value where the B/M ratio is at its maximum will increase with collision centrality. This prediction can be compared to the Λ/K_S^0 data. Measurements are still not precise enough, however, to confirm nor disprove this prediction. Figure 1 demonstrates that the baryon enhancement in Au+Au collisions is part of a systematic trend. Baryon production is also enhanced in $\sqrt{s} = 10$ GeV e^+e^- collisions when $e^+e^- \rightarrow \Upsilon \rightarrow ggg$ events are compared to continuum $e^+e^- \rightarrow q\bar{q}$ events [12]. From those measurements the question arose: *is the enhancement related to multi-parton topological effects or a difference between quark and gluon fragmentation?* Since $e^+e^- \rightarrow \Upsilon \rightarrow ggg$ is a purely gluonic process, the observation that the \bar{p}/π^- ratio is even larger in Au+Au collisions indicates that multi-parton topological effects drive the enhancement (baryon junctions or coalescence).

2.1. Azimuthal Dependence: v_2

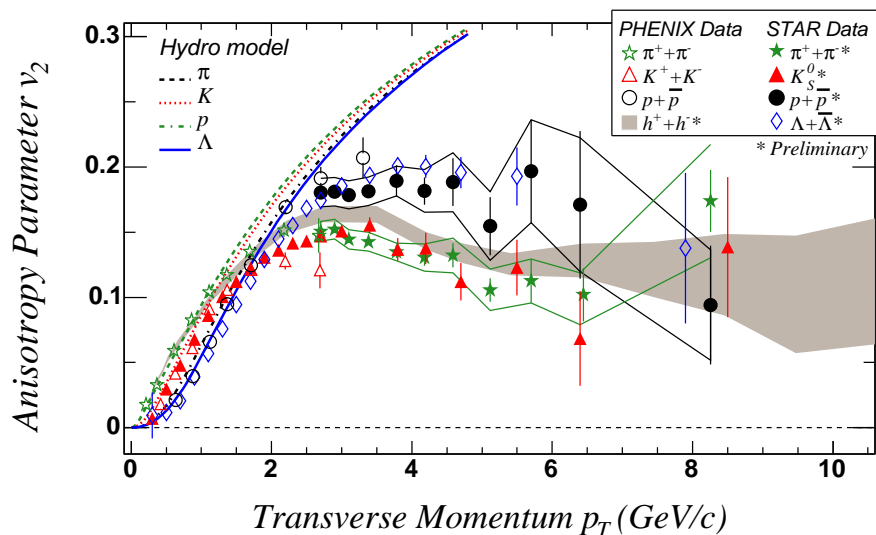


Figure 2. Elliptic flow measurements at middle rapidity from minimum-bias Au+Au collisions at $\sqrt{s_{NN}} = 200$ GeV. The bands around the STAR preliminary measurements of pions and protons represent systematic uncertainties mostly from non-flow correlations. The PHENIX measurements are made by correlating hadrons at middle rapidity with an event-plane measured using hadrons at $3.1 < |\eta| < 4.0$.

v_2 is a sensitive measure to distinguish between possible interpretations of the hadron type dependence of particle spectra. Figure 2 shows preliminary measurements of v_2 with a minimum bias centrality selection in Au+Au collisions at $\sqrt{s_{NN}} = 200$ GeV [15, 16]. The curves show v_2 for pions, kaons, protons and Λ s from a hydrodynamic calculation [9]. At $p_T < 1.0$ GeV/c, the mass ordering suggests that v_2 in that region results from collective motion. The hydrodynamic calculations capture some of the general features of the data in this region. At much higher p_T it is expected

that v_2 will be developed via energy loss by fast partons as they traverse the medium created in the collisions. Calculations suggest that v_2 from this mechanism should be less than 10% [17]. It is also expected that all hadrons will have similar v_2 values where partonic energy loss is the dominant source of v_2 . The magnitude and particle-type dependence of v_2 seen for $p_T < 6$ GeV/c suggests that other mechanisms contribute to the development of v_2 up to 6–7 GeV/c. This observation is consistent with results from a parton cascade model predicting that the effects of flow may persist up to $p_T = 7$ GeV/c [18]. At $p_T = 7$ GeV/c, within errors, the particle-type dependence of v_2 disappears and the v_2 measurements are consistent with expectations from energy loss models [17].

2.2. Quark Number Dependence

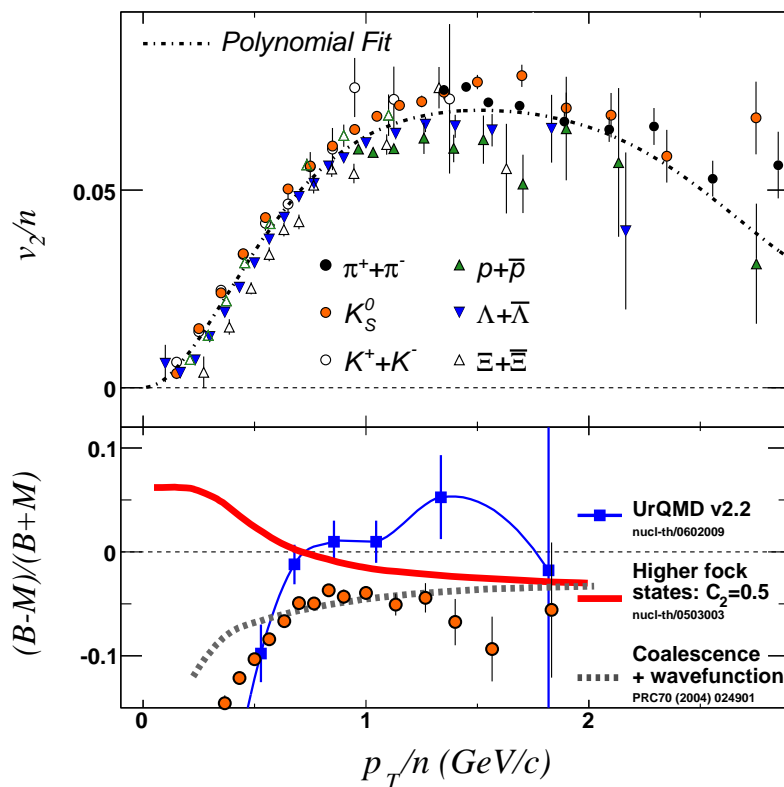


Figure 3. Top panel: Quark number scaled elliptic flow for identified hadrons (Preliminary) [15, 16]. A polynomial is fit to all data points. Bottom panel. The difference between quark number scaled baryon v_2 and quark number scaled meson v_2 divided by the sum: $(B - M)/(B + M)$. Here the ratio is taken using $\Lambda + \bar{\Lambda}$ and K_S^0 . Model predictions are also shown on the lower panel. The model that provides the best description of the data is the recombination model that takes the wave-function of the hadron into account. Kaon and Λ data were used for the UrQMD model comparison.

Hadronization by coalescence or recombination of constituent quarks is thought to explain many features of hadron production in the intermediate p_T region ($1.5 < p_T < 5$ GeV/c) [6]. These models find that at intermediate p_T , v_2 may follow a quark-number (n_q) scaling with $v_2(p_T/n_q)/n_q$ for all hadrons falling on one curve. This scaling behavior has been observed in Au+Au collisions at 200 GeV [5]. More sophisticated theoretical considerations have led to predictions of fine structure in quark-number scaling—with predictions for a baryon v_2/n_q being smaller than meson v_2/n_q [19, 20]. Figure 3 (top panel) shows v_2 vs p_T for identified particles, where v_2 and p_T have been scaled by n_q . A polynomial function is fit to the scaled values. The deviations from the scaling are shown

in the bottom panel by plotting the difference between the scaled baryon v_2 and the scaled meson v_2 divided by the sum $(B - M)/(B + M)$. Theoretical predictions for this value are also shown. The model that compares best to data is a coalescence model that includes the effect of quark momentum distributions inside the hadron (*Coalescence + wavefunction*) [19]. Accounting for the substructure of constituent quarks (*higher fock states*) [20] leads to a negative $(B - M)/(B + M)$ ratio but with a smaller magnitude than observed in the data. The hadron/string model UrQMD yields v_2 values smaller by a factor of two than experimental data. The model does, however, find a scaling with quark number. In this model the scaling originates from the additive quark model for hadronic cross-sections. It should be noted, when considering comparisons to any models, that the systematic uncertainties on these preliminary measurements have not yet been specified.

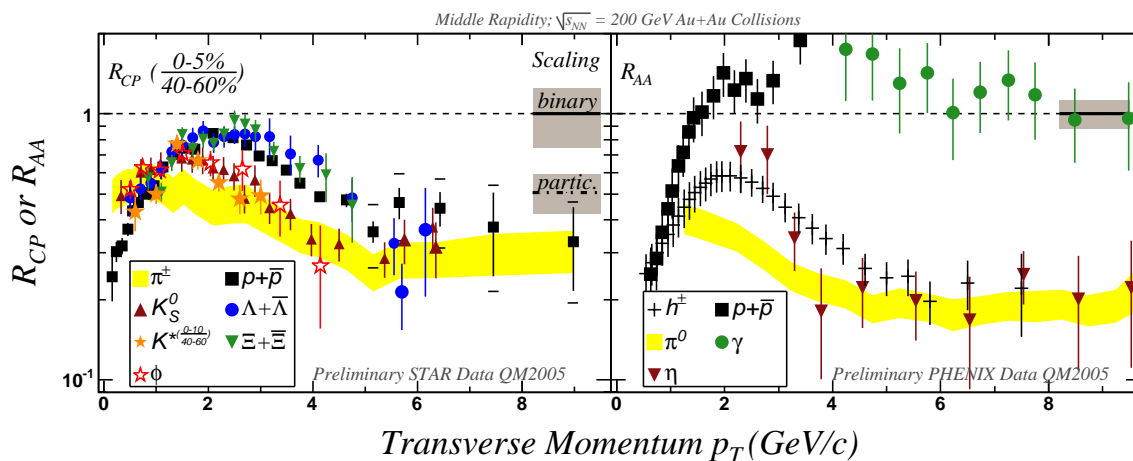


Figure 4. Preliminary identified particle R_{CP} (left panel) and R_{AA} (right panel). Grey bands represent the error on the N_{bin} and N_{part} calculations. For the R_{AA} data, error bars represent both systematic and statistical uncertainties. For pion R_{CP} , the yellow band includes both systematic and statistical uncertainties. For proton R_{CP} , the systematic uncertainties are shown as brackets on the final five points (systematic uncertainties are similar for lower p_T points).

Quark-number dependences at intermediate p_T are also manifested in the centrality dependence of the p_T spectra. Figure 4 shows the ratios R_{CP} [3, 22, 13, 23] (central Au+Au over peripheral Au+Au) in the left panel and R_{AA} [24, 25] (Au+Au over p+p) in the right panel where the spectra have been scaled by the number of binary nucleon-nucleon collisions (N_{bin}). For $p_T > 1.5$ GeV/c, R_{CP} values are grouped by hadron type (mesons vs. baryons). The larger baryon R_{CP} values indicate that baryon production increases more quickly with centrality than meson production. This observation is confirmed with good precision for protons and hyperons. The ϕ is a particularly interesting test particle since it is a meson but is more massive than the proton. With good precision, the ϕ is now confirmed to follow the systematics of the other mesons.

Measurement of K_S^0 and $\Lambda + \bar{\Lambda}$ R_{CP} at $\sqrt{s_{NN}} = 17.2$ GeV indicate that baryon production is also enhanced at lower center-of-mass energies [26]: with $\Lambda + \bar{\Lambda}$ R_{CP} values

well above N_{bin} scaling. The difference between $\Lambda + \bar{\Lambda} R_{CP}$ and $K_S^0 R_{CP}$ is similar at all energies. This similarity is surprising since the underlying shape of the spectrum is changing very drastically with $\sqrt{s_{NN}}$, becoming much steeper at higher energies. It remains to be seen if any of the current theoretical interpretations of the baryon enhancement can explain this lack of energy dependence in the relative enhancement of baryons.

3. Implications for non-photonic electron R_{AA}

If the baryon enhancement also exists for charm hadrons, then the non-photonic electron spectrum may be affected [27]. The branching ratio for $\Lambda_c \rightarrow e + \text{anything}$ ($4.5\% \pm 1.7\%$) is smaller than that for $D^\pm \rightarrow e + \text{anything}$ ($17.2\% \pm 1.9\%$) or $D^0 \rightarrow e + \text{anything}$ ($6.87\% \pm 0.28\%$) [28]. In this case, even if charm quark production is unchanged, increasing the Λ_c/D ratio will lead to a reduction in the number of observed non-photonic electrons. In Fig. 5 (left) we show the effect of a Λ_c enhancement on the charm decay electron spectrum. The ratio of two cases is taken: Λ_c/D follows the shape of the Λ/K_S^0 ratio in Au+Au collisions, or it follows the shape of the Λ/K_S^0 ratio in p+p collisions. A suppression of electrons from heavy flavor decays due to the larger charm baryon-to-meson ratio in Au+Au collisions is visible. The suppression in this figure is a result of smaller $\Lambda_c \rightarrow e + \text{anything}$ branching ratio. The different curves show the experimental uncertainties on the branching ratio [28]. The figure demonstrates that even if the total charm yield follows N_{bin} scaling, the non-photonic electron spectrum can be suppressed. The magnitude of the suppression depends on the Λ_c/D ratio and the $\Lambda_c \rightarrow e + \text{anything}$ branching ratio. The Λ_c/D ratio in Au+Au collisions is unknown but for the charm baryon-to-meson ratio assumed here, the suppression can be as large as 20%. In Fig. 5 (right) we show the case when charm R_{AA} follows light quark R_{AA} and Λ_c is enhanced. The non-photonic electron data are above the resulting non-photonic electron curve. If we scale the input charm R_{AA} up and calculate the χ^2 , we find the smallest χ^2 value for charm quark $R_{AA} = 1.35 \times$ charged hadron R_{AA} .

4. Interpretation of pion R_{AA}

It has been proposed that the large B/M values at RHIC may be a result of the suppression of pion production coupled with novel baryon production mechanisms scaling with N_{bin} or N_{part} [8]. The lower energy measurements call this interpretation into question since baryon production is still enhanced even while the suppression of mesons is much weaker. Furthermore, it is possible that part of the pion suppression is actually a manifestation of the baryon enhancement. Most baryons do not decay into pions while many meson resonances do. If the relative fraction of baryons is increasing with centrality, then that should lead to an absence of pions from decays. Much of the difference between Kaon and pion R_{AA} [25, 13] may be caused by this effect: an effect exactly analogous to that described in the previous section on non-photonic electrons.

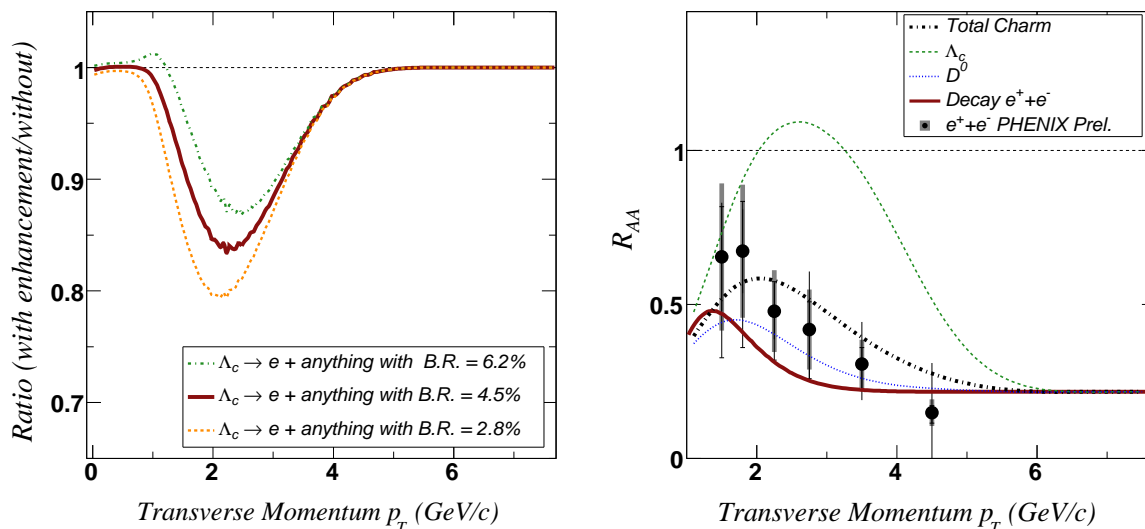


Figure 5. Left panel: Electron spectrum with Λ_c enhancement divided by the spectrum without Λ_c enhancement. Right panel: R_{AA} for charm hadrons and non-photon electrons. The total charm spectrum in Au+Au collisions is scaled by the charged hadron R_{AA} values. In this way the total charm hadron R_{AA} has the same form as the charged hadron R_{AA} . The Λ_c/D ratio is given the same form as the preliminary Λ/K_S^0 ratio. For $p_T < 6$ GeV/c, the resulting decay electron R_{AA} is smaller than either the D -meson or total charm R_{AA} .

5. Conclusions

Pion, kaon, proton, and hyperon momentum-space distributions have been measured up to $p_T \approx 10$ GeV/c. Several observations indicate that at $p_T > 6$ GeV/c, hard processes may dominate particle production. Below this, measurements of the B/M ratios, R_{CP} , and v_2 indicate that processes beyond the reach of perturbative QCD are prevalent. The baryon enhancement at intermediate p_T is seen to be generic to many systems and appears to be correlated with higher multiplicity. Measurements favor pictures involving multi-parton dynamics and point to the presence of active quark and gluon degrees-of-freedom. A baryon enhancement in the charm sector is shown to potentially impact the interpretation of non-photon electron R_{AA} . For the scenario presented we find that preliminary non-photon electron R_{AA} data prefer a charm quark R_{AA} 35% larger than light quark R_{AA} . We also note that the baryon enhancement may lead to an extra suppression of pions due to the reduction in the number of pions from resonance decays when baryon production becomes preferred.

Acknowledgments

I thank the conference organizers and acknowledge valuable input from H. Huang, Z. Xu, H. Long, J. Nagle, X. Dong, N. Xu, H-G. Ritter, S. Blyth, M. Oldenburg, J. Chen, and Y. Lu. I also thank the Battelle Memorial Institute and Stony Brook University for

support in the form of the Gertrude and Maurice Goldhaber Distinguished Fellowship.

References

- [1] I. Arsene *et al.* [BRAHMS Collaboration], Nucl. Phys. A **757**, 1 (2005);
B.B. Back *et al.* [PHOBOS Collaboration], Nucl. Phys. A **757**, 28 (2005);
J. Adams *et al.* [STAR Collaboration], Nucl. Phys. A **757**, 102 (2005);
K. Adcox *et al.* [PHENIX Collaboration], Nucl. Phys. A **757**, 184 (2005).
- [2] S. S. Adler *et al.* [PHENIX Collaboration], Phys. Rev. Lett. **91**, 172301 (2003).
- [3] J. Adams *et al.* [STAR Collaboration], Phys. Rev. Lett. **92**, 052302 (2004).
- [4] P. R. Sorensen, J. Phys. G **31**, S889 (2005); P. R. Sorensen, arXiv:nucl-ex/0309003.
- [5] J. Adams *et al.* [STAR Collaboration], Phys. Rev. C **72**, 014904 (2005).
- [6] D. Molnar and S. A. Voloshin, Phys. Rev. Lett. **91**, 092301 (2003); R. C. Hwa and C. B. Yang, Phys. Rev. C **67**, 064902 (2003); R. J. Fries, B. Muller, C. Nonaka and S. A. Bass, Phys. Rev. C **68**, 044902 (2003); V. Greco, C. M. Ko and P. Levai, Phys. Rev. C **68**, 034904 (2003);
- [7] D. Kharzeev, Phys. Lett. B **378**, 238 (1996); S. E. Vance, M. Gyulassy and X. N. Wang, Phys. Lett. B **443**, 45 (1998).
- [8] I. Vitev and M. Gyulassy, Nucl. Phys. A **715**, 779 (2003).
- [9] P. Huovinen, P. F. Kolb, U. W. Heinz, P. V. Ruuskanen and S. A. Voloshin, Phys. Lett. B **503**, 58 (2001).
- [10] M. Shao, O. Barannikova, X. Dong, Y. Fisyak, L. Ruan, P. Sorensen and Z. Xu, arXiv:nucl-ex/0505026;
E. Kistenev [PHENIX Collaboration], AIP Conf. Proc. **698**, 775 (2004).
- [11] A. Sickles [PHENIX collaboration], J. Phys. G **30**, S1291 (2004); S. S. Adler *et al.* [PHENIX Collaboration], Phys. Rev. C **71**, 051902 (2005).
- [12] H. Albrecht *et al.* [ARGUS Collaboration], Z. Phys. C **44**, 547 (1989).
- [13] O. Y. Barannikova, arXiv:nucl-ex/0505021; L. Ruan, arXiv:nucl-ex/0503018.
- [14] J. Adams *et al.* [STAR Collaborations], “Measurements of identified particles at intermediate transverse momentum in arXiv:nucl-ex/0601042.
- [15] J. Adams *et al.* [STAR Collaboration], Phys. Rev. Lett. **95**, 122301 (2005). M. Oldenburg [the STAR Collaboration], arXiv:nucl-ex/0510026.
- [16] H. Masui, arXiv:nucl-ex/0510018.
- [17] R. Baier, D. Schiff and B. G. Zakharov, Ann. Rev. Nucl. Part. Sci. **50**, 37 (2000); M. Gyulassy, I. Vitev, X. N. Wang and B. W. Zhang, arXiv:nucl-th/0302077.
- [18] D. Molnar, arXiv:nucl-th/0503051.
- [19] V. Greco and C. M. Ko, Phys. Rev. C **70**, 024901 (2004).
- [20] B. Muller, R. J. Fries and S. A. Bass, Phys. Lett. B **618**, 77 (2005).
- [21] Y. Lu *et al.*, arXiv:nucl-th/0602009.
- [22] J. Adams *et al.* [STAR Collaboration], Phys. Lett. B **612**, 181 (2005); J. Adams *et al.* [STAR Collaboration], Phys. Rev. C **71**, 064902 (2005).
- [23] J. C. Dunlop [STAR Collaboration], arXiv:nucl-ex/0510073.
- [24] S. S. Adler *et al.* [PHENIX Collaboration], Phys. Rev. C **69**, 034909 (2004).
- [25] M. Csanad [PHENIX Collaboration], arXiv:nucl-ex/0505001; M. Konno [PHENIX Collaboration], arXiv:nucl-ex/0510022; M. Shimomura, arXiv:nucl-ex/0510023.
- [26] A. Dainese, arXiv:nucl-ex/0510001; F. Antinori *et al.* [NA57 Collaboration], Phys. Lett. B **623**, 17 (2005).
- [27] P. R. Sorensen and X. Dong, arXiv:nucl-th/0512042.
- [28] S. Eidelman *et al.* [Particle Data Group], Phys. Lett. B **592**, 848 (2004).